

High-Operating-Temperature MWIR Detector Diodes

H.F. SCHAAKE,^{1,2} M.A. KINCH,¹ D. CHANDRA,¹ F. AQARIDEN,¹
P.K. LIAO,¹ D.F. WEIRAUCH,¹ C.-F. WAN,¹ R.E. SCRITCHFIELD,¹
W.W. SULLIVAN,¹ J.T. TEHERANI,¹ and H.D. SHIH¹

1.—Infrared Technologies Division, DRS Sensors & Targeting Systems, Inc, P.O. Box 740188, Dallas, TX 75374, USA. 2.—e-mail: hfschaake@drs-irtech.com

The high-operating-temperature (HOT) midwave infrared (MWIR) *n-on-p* detector has been pursued using the high-density vertically integrated photodiode (HDVIP[®]) architecture. In this device, arsenic-doped HgCdTe grown by liquid-phase epitaxy (LPE) is used, passivated on both surfaces with interdiffused CdTe. Dark current densities on these diodes as low as 2.5 mA/cm² normalized to a 5 μm cutoff at 250 K have been demonstrated. 1/*f* noise at 1 Hz, measured at 250 K, is found to be 6 × 10⁻¹¹ A/rHz-cm measured on a cutoff of 4.43 μm. These results agree with the theoretical predictions for the devices made.

Key words: HgCdTe, high-operating-temperature photodiodes, arsenic-doped HgCdTe

INTRODUCTION

The operation of midwave infrared (MWIR) focal-plane arrays at elevated temperatures enables substantial reductions in the size, weight, and power consumption of the coolers used to refrigerate the arrays. At suitably high operating temperatures, ~220 K, the use of inexpensive thermoelectric coolers and simpler Dewar packaging become practical. The achievement of these improved designs opens up the possibility of totally new applications in surveillance and threat warning.

The HOT detector, originally proposed by Ashley and Elliott¹ is a reverse-biased photodiode with minority and majority carrier contacts. The active volume, which is less than a diffusion volume, is in nonequilibrium due to the reverse bias, and the intrinsic thermally generated minority carriers are fully extracted through the minority carrier contacts. Charge neutrality in the active volume is lost, setting up electric fields within the diode. The majority carriers are then swept out through the majority carrier contacts until the remaining majority carrier concentrations equal the background doping concentrations on either side of the

junction. The reduction in majority and minority carrier concentrations in the active volume of the HOT device results in a significant reduction in the dark current generation rates in that volume, with the potential for background-limited infrared performance (BLIP) performance at or near room temperature. Detailed considerations show that the primary sources of dark current in these devices will be dominated by recombination via Shockley-Read-Hall defects or by the Auger mechanism.² For similar majority carrier concentrations, the Auger7 recombination lifetime, which is dominant in *p*-type HgCdTe, is ~6 times that of the Auger1 lifetime that dominates in *n*-type HgCdTe.³ Thus the configuration for a HOT detector having the lowest dark current at a given temperature is one in which infrared radiation is detected in a lightly doped *p*-region.

In this paper, we report on results obtained on MWIR HOT detectors based on DRS' HDVIP[®] architecture.⁴ A unit cell of this detector, along with a conventional HDVIP unit cell, is shown schematically in Fig. 1. The conventional HDVIP unit cell, shown in Fig. 1a is an *n⁺/n⁻/pp⁺* structure. The *n⁻* and *n⁺* regions form during the electron cyclotron resonance (ECR) etching of the via to interconnect the diode to the underlying read-out integrated circuit (ROIC). The *n⁻* doping reflects the background

(Received November 6, 2007; accepted February 20, 2008; published online March 21, 2008)

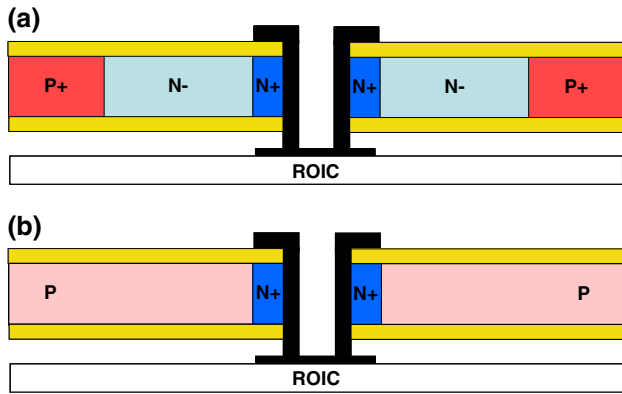


Fig. 1. Schematic cross-sections through a HDVIP diodes. (a) Conventional diode architecture. (b) HOT architecture.

indium concentration that is introduced during the LPE growth of the HgCdTe. The p^+ results from both copper and metal vacancies introduced into the HgCdTe during the passivation of the two surfaces of the HgCdTe. The HOT structure, shown in Fig. 1b, is basically an n^+/p diode. The p -side of the diode arises from arsenic doping during the LPE growth of the HgCdTe films from a tellurium-rich melt. After growth, the arsenic in the film, typically $1 \times 10^{15} \text{ cm}^{-3}$ to $2 \times 10^{15} \text{ cm}^{-3}$, is activated as an acceptor by a high-temperature 400°C to 425°C anneal in a mercury-rich ambient. Thin films of the HgCdTe are then passivated with CdTe, interdiffused at 250°C . The interdiffusion process also introduces metal vacancies into the film at a level of $\sim 1 \times 10^{16} \text{ cm}^{-3}$. ECR etching used to form the vias used to interconnect the n -side of the detector to the ROIC below injects mercury interstitials into the HgCdTe. These interstitials annihilate the metal vacancies in the HgCdTe, and also react with the arsenic on the tellurium sublattice, producing donor complexes. Ion implantation into the sidewall stabilizes the n^+ region of the diode and provides additional mercury interstitials to fill vacancies during subsequent baking. Low-temperature baking of the structure then destroys the arsenic-mercury interstitial complexes, converting the bulk of the HgCdTe back to p -type.

TESTING AND RESULTS

For the work reported here, HDVIP mini-arrays, shown in Fig. 2, were used. These are 4×4 arrays of HDVIP diodes and are most convenient for measuring diode I - V behavior. The innermost four pixels are connected together and form the test diode to be measured. The outer ring of pixels are separately joined together and function as a guard diode. A test bar contains a number of these mini-arrays, each having a different via diameter and/or pixel pitch. Pitches range from $15 \mu\text{m}$ to $40 \mu\text{m}$. In most of the work reported here, the guard diodes were kept at a constant reverse bias of 600 mV as the test diode

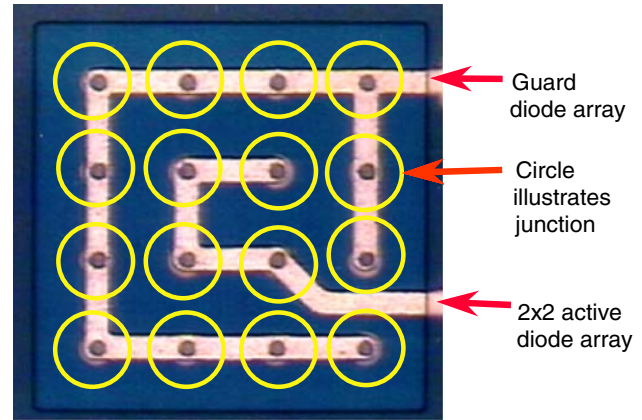


Fig. 2. HDVIP mini-array on a test bar. A test bar contains mini-arrays having different via diameters and pixel pitches.

was swept through a bias range of -400 mV to $+800 \text{ mV}$. Because of the constant guard diode bias, the thermally generated carriers are always swept out of the array, and a decrease in dark current with the initial biasing of the test diode is not observed. The HgCdTe material used did show some variation in the cutoff and the thickness, both of which directly affect the dark current. In order to compare the results of different material and process variations directly, the dark currents were normalized to a cutoff of $5 \mu\text{m}$ at 250 K , and to a material thickness of $3 \mu\text{m}$ by taking the dark current density to be proportional to the thickness of the HgCdTe, and to the square of the intrinsic carrier concentration.²

Figure 3 shows the I - V curves measured at 200 K on test bar D4827.1. The material in the test bar was doped with $1.5 \times 10^{15} \text{ cm}^{-3}$ arsenic, had a thickness of $2.34 \mu\text{m}$, and a 77 K cutoff of $5.175 \mu\text{m}$, corresponding to a cutoff of $4.43 \mu\text{m}$ at 250 K . Figure 3a shows the I - V curves of all mini-arrays on the test bar immediately after fabrication, before any arsenic decomplexing bake. The structure of the diodes in these arrays is expected to be $n^+/n^-/p^+$, as depicted in Fig. 1a. The n^- concentration is determined by the number of arsenic-mercury interstitial complexes present, $1.5 \times 10^{15} \text{ cm}^{-3}$ in these diodes. The dark current density measured, 1 mA/cm^2 in most mini-arrays, corresponds to a normalized dark current density $>50 \text{ mA/cm}^2$ at 250 K . These dark currents are typical of those that were measured in vacancy-only material.

After baking the test bar for 5 days at 120°C , the I - V curves shown in Fig. 3b were measured. Dark current densities as low as $24 \mu\text{A/cm}^2$ were measured, corresponding to a value of 2.6 mA/cm^2 normalized to a $5 \mu\text{m}$ cutoff at 250 K . The diode structure has been converted to that shown in Fig. 1b. The dark current density clearly arises from a diffusion mechanism. Its value is in agreement with the dark current predicted for the Auger7 mechanism, $\sim 17 \mu\text{A/cm}^2$, for this doping level and cutoff, using the theoretical Auger7 lifetime.³

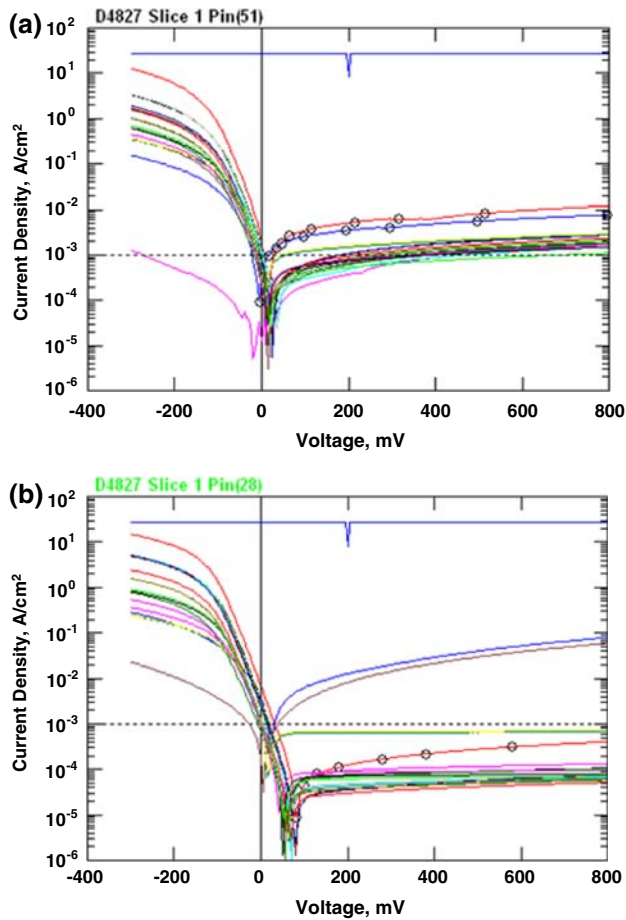


Fig. 3. I - V curves of mini-arrays on test bar D4827.1 measured at 200 K. The mini-arrays have pitches ranging from 15 μm to 40 μm , and via diameters ranging from 4 μm to 10 μm . (a) I - V curves prior to decomplexing bake. (b) After decomplexing bake at 120°C.

An interesting feature of the I - V curves in Fig. 3b in comparison with those of Fig. 3a is that they are offset from the zero bias point. This is an indication that the test diode is coupled to the guard diode as a result of very long diffusion lengths, $>100 \mu\text{m}$, in the bulk of the material. The offset is not observed when the guard diode bias tracks the test diode bias, rather than being held fixed at 600 mV.

I - V curves for one of the mini-arrays on this test bar as a function of temperature are shown in Fig. 4a. The dark current densities are plotted against the intrinsic carrier concentration, n_i ,⁵ in Fig. 4b. The dark current densities are found to vary as $n_i^{1.85}$, slightly less than the anticipated n_i^2 . This may be due to a small contribution to the dark current from a small number of residual metal vacancies. The bias offset of this diode increases with increasing temperature (Fig. 4a). This correlates with an increase in the lifetime with temperature, resulting in an increased coupling between the test diode and the guard diode.

The evolution of the standard structure shown in Fig. 1a to the HOT structure shown in Fig. 1b has been followed and is illustrated in Fig. 5. The

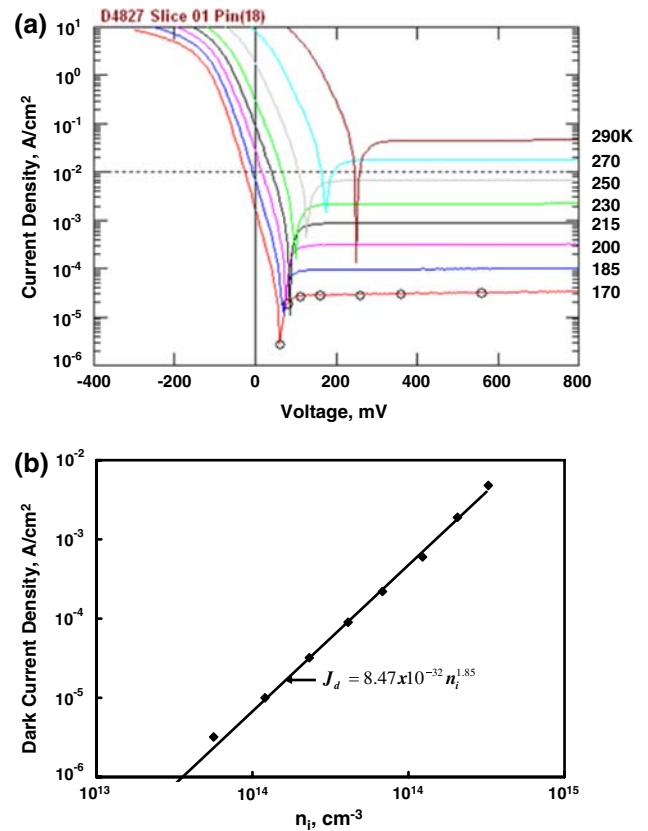


Fig. 4. Dark current density in a 30- μm -pitch 10- μm -via mini-array on test bar D4827.1 at various temperatures. This test bar had a HgCdTe thickness of 2.34 μm and a 77 K cutoff of 5.175 μm , corresponding to a cutoff of 4.43 μm at 250 K. (a) I - V curves. (b) Dark current density versus intrinsic carrier concentration, n_i .

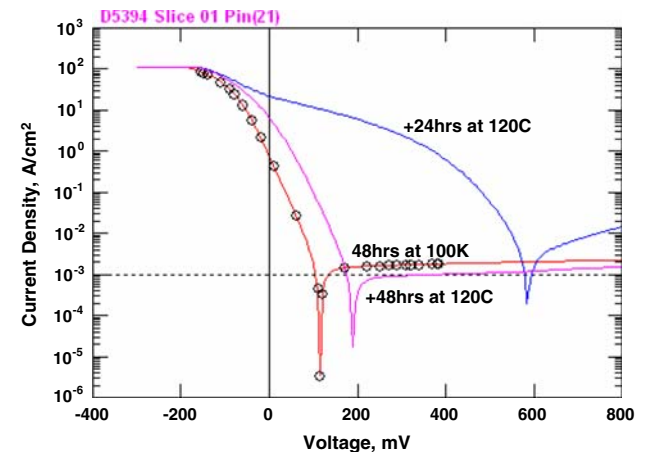


Fig. 5. I - V curves of the 15- μm -pitch, 3- μm -via mini-array on test bar D5394.1 measured at 200 K. The HgCdTe had a cutoff of 5.31 μm at 77 K, corresponding to a cutoff of 4.75 μm at 200 K and 4.37 μm at 300 K, and a thickness of 4.12 μm . The arsenic concentration in the HgCdTe was $\sim 1.5 \times 10^{15} \text{ cm}^{-3}$. The reported values of the dark current densities are elevated by leakage caused by the propanol into which the sample was immersed. The dark current density measured in a Dewar at the conclusion of the second 120°C bake is a factor of 4.5 lower than that measured while immersed in propanol.

interpretation of this sequence of I - V curves is as follows:

- (1) At the completion of normal processing followed by the 48 h bake at 100°C the diode has the standard structure shown Fig. 1a.
- (2) Baking for an addition 24 h at 120°C results in the emission of additional mercury interstitials from the sidewall implant. These interstitials annihilate most of the metal vacancies, but suppress the breakup of the arsenic-mercury interstitial complexes. This results in diodes that are shunted through the bulk of the HgCdTe due to the n -type behavior of the mercury interstitial-arsenic complexes.
- (3) An additional 24 h bake at 120°C results in the breakup of mercury-interstitial-arsenic complexes and the unshunting of the diodes. The HOT structure of Fig. 1b is being approached, although some arsenic-mercury interstitial complexes probably remain.

The dark current density in this array is a factor of ~ 4 larger than that predicted by either an Auger7 or an Auger1 recombination mechanism. A possible explanation for this discrepancy may lie in the fact that the guard ring diodes do not completely shield the test diode from the remaining bulk of the HgCdTe. Figure 6 shows a response map of a spot scan of the test diode in a mini-array on this test bar. There is considerable response outside of the guard diode region. The current collected from outside of the guard diode region represents half of the dark current collected from within the mini-array itself. In the test bar case, this means that some dark current from vacancies that were not annihilated at some distance from the mini-array can still

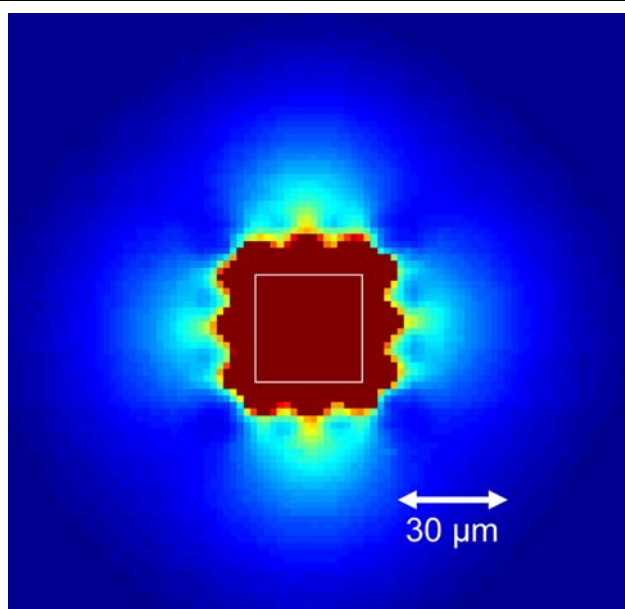


Fig. 6. Spot scan response map of the 15- μ m-pitch 4- μ m-via mini-array on test bar D5394.1, measured at 300 K.

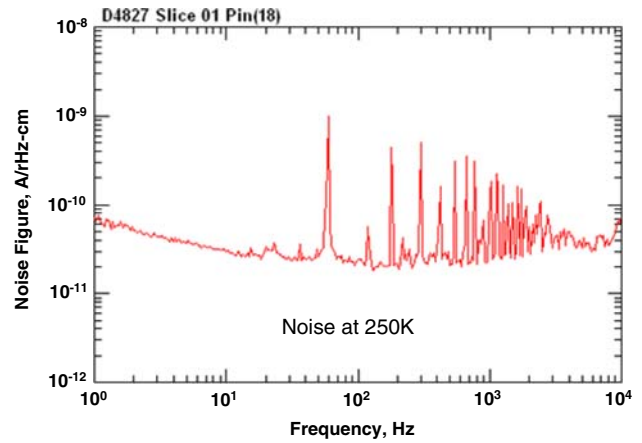


Fig. 7. Noise measured at 250 K in Test Bar D4827.1. At 1 Hz, the $1/f$ noise is 6×10^{-11} A/rHz-cm.

be collected by the imperfectly shielded test diode and possibly give rise to the higher dark current that is observed. An improved test structure is being implemented to prevent this possibility.

Spectral noise measurements have also been made in some of these devices. At 250 K the magnitude of the $1/f$ noise in test bar D4827.1 is 6×10^{-11} A/rHz-cm at 1 Hz, as shown in Fig. 7. The measurements agree with the noise model of Schiebel,⁶ which predicts that the $1/f$ noise arises from surface-modulated diffusion currents when the dislocation density is low ($< 2 \times 10^9/\text{cm}^2$). The $1/f$ noise is then predicted to vary as the square root of the trap density in the passivation interface, $N_T^{1/2}$. The $1/f$ modulation of dark currents has been measured and modeled for the DRS standard CdTe passivation process. They have been found to be consistent with a surface trap density of $\sim 10^{12} \text{ cm}^{-2}$, as shown in Fig. 8. For the dark current density measured in test bar D4827.1 ($600 \mu\text{A}/\text{cm}^2$), the Schiebel model predicts 3.2×10^{-11} A/rHz-cm at 1 Hz, close to the measured value.

DISCUSSION

The results to date demonstrate that the goal of obtaining high-operating-temperature devices has been met. Dark current densities near to those expected for the arsenic doping levels used frequently have been achieved. It is suspected that the incomplete annihilation of metal vacancies during processing is one major cause for failure to reach the lowest dark currents.

A second failure mechanism that has been observed is surface shunting, which leads to extremely high dark currents. The shunting arises from fixed positive charge at the passivation-HgCdTe interface. This charge, when sufficiently large, results in the inversion of the surface HgCdTe, leading to surface shunting of all of the diodes in the array. The susceptibility of the HgCdTe to the formation of this inversion layer increases as the concentration

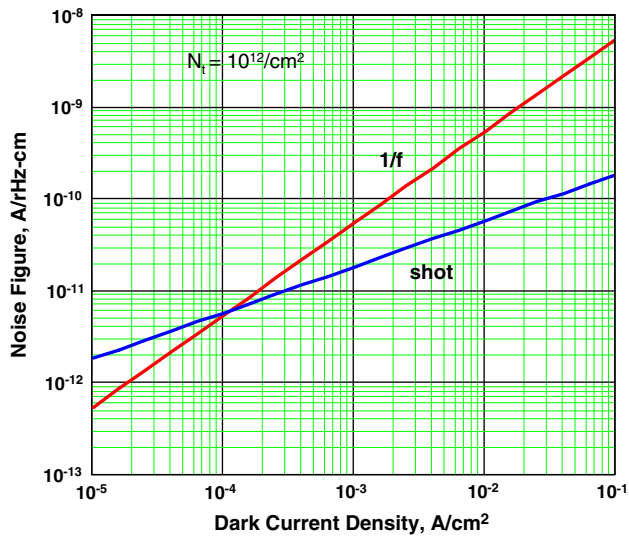


Fig. 8. Predictions of the Schiebel⁶ model for the $1/f$ noise for a surface trap density of 10^{12} cm^{-2} . The dark current shot noise is also shown.

of the p -type dopant decreases. Thus limiting the level of this charge in the passivation is necessary to be able to use the lower arsenic doping. On-going

work on this problem indicates that the charge in the passivation is a result of impurities that are introduced into the passivation during the interdiffusion process. Chlorine is one impurity strongly implicated by secondary ion mass spectrometry (SIMS) measurements.

One of our next efforts will be to reduce the arsenic doping level to $\sim 2 \times 10^{14} \text{ cm}^{-3}$. This should enable the dark current densities to be reduced to $< 500 \mu\text{A}/\text{cm}^2$ at 250 K and 5 μm cutoff.

ACKNOWLEDGEMENT

This material is based on work supported by the Defense Advanced Research Projects Agency (DARPA) under Contract No. NBCHC06001. The DARPA Program Manager is Ray Balcerak.

REFERENCES

1. T. Ashley and C.T. Elliott, *Electron. Lett.* 21, 451 (1985).
2. M.A. Kinch, *Proc. SPIE* 4454, 21 (2001).
3. S. Krishnamurthy and T.N. Casselman, *J. Electron. Mater.* 29 (2000).
4. M.A. Kinch, *Proc. SPIE* 4369, 566 (2001).
5. G.L. Hansen and J.L. Schmit, *J. Appl. Phys.* 54, 1639 (1983).
6. R.A. Schiebel, *IEEE Trans. Electron. Dev.* ED-41, 768 (1994).